

Comparison between the assimilation of IASI Level 2 retrievals and Level 1 radiances for ozone reanalyses. Reply to referee # 1

Emanuele Emili¹, Brice Barret², Eric Le Flochmoën², and Daniel Cariolle¹

¹CECI, Université de Toulouse, Cerfacs, CNRS, Toulouse, France

²Laboratoire d'Aérodynamique, Université de Toulouse, CNRS, UPS, Toulouse, France

Correspondence: Emili (emili@cerfacs.fr)

1 Reply to general comments

We thank the anonymous reviewer for his comments, which helped to improve significantly the manuscript. Detailed replies to his comments follow:

1. *Although both SOFRID retrievals and assimilation of L1 use the RTTOV model, differences may be significant. Indeed the version of the RTTOV coefficients used in both cases is not given. I suspect that SOFRID uses coefficients on 43 levels which are the levels of the retrieval and that the L1 assimilation uses newer coefficients, on 54 or 101 levels (the authors state 104 vertical levels on P7 L20 which does not exist), which may have been build from a different line-by-line model (or different version of that model; or even from a different spectroscopic database). Such differences can have visible impacts on the radiance simulation by RTTOV. Could the authors give more details about the coefficients? Is it possible to produce SOFRID L2 retrievals using the same version of RTTOV model and RTTOV coefficients as those used in CTM assimilation? And then run the L2 assimilation trials in CTM? That would be a significant improvement to the comparison proposed in this paper!*

Answer:

A verification of the differences between the versions of RTTOV used for this study (v9 for SOFRID and v11.3 for L1 assimilation) confirmed the concerns of the reviewer: SOFRID retrievals were based on a mixture of HITRAN 2000 and 2004 spectroscopic databases, LBLRTM v11.1 radiative transfer and predictors computed for 43 levels, whereas L1 assimilation uses HITRAN 2008, LBLRTM v12.2 and predictors on 101 vertical levels. Therefore, we switched to an updated version of SOFRID and recomputed L2 retrievals with RTTOV 11.1 and the same predictors used for L1 assimilation (101 levels). Other minor differences between RTTOV 11.1 and 11.3 do not impact the radiance computations. New L2 retrievals using RTTOV 11 are named v3.0, as opposed to v1.6 used for the original manuscript. A short summary of the different versions of SOFRID used for this study is given in Tab. 1. The further assimilation of v3.0 retrievals confirmed the results observed previously at tropical latitudes but reduced significantly the differences between L1a and L2a in the Southern Hemisphere mid-latitudes (Fig. 1 and 2). We conclude that the interpretation of the results in the

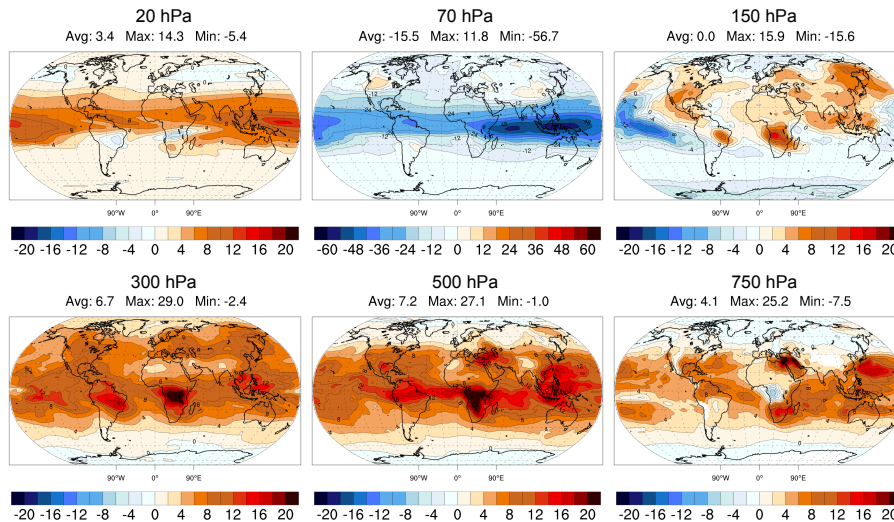


Figure 1. Relative differences (%) between radiances and Level 2 assimilation (L1a minus L2a divided by the correspondent O_3 values of the control simulation) averaged on July 2010. From left to right different pressure levels are displayed covering the stratosphere (top) and the free troposphere (bottom). Average, maximum and minimum values of the displayed fields are given on top of each map. The same pixels selection of the original manuscript is used to produce this figure. The only difference with the original manuscript is that SOFRID v3.0 retrievals are used instead of v1.6 (Tab. 1)

SH mid-latitudes given in the original manuscript was not correct: the L1 assimilation does not reduce the biases when the instrument's sensitivity is low thanks to a better prior. The better performances of L1a in the SH mid-latitudes were mostly due to improved radiative transfer computations.

These findings made us revise the discussion of the results (Sec. 4.1 and 4.3 of the revised manuscript) and, partly, the conclusions. Even if the positive results of the original manuscript are somehow mitigated in the SH, the main conclusions remain valid elsewhere. Moreover, we can now provide a more satisfactory explanation of the differences between L1a and L2a: large differences arise only where the model departures from the SOFRID prior are very large (> 100%), i.e. at low latitudes (< 40°). As the second referee also pointed out, differences between L1a and L2a do not really depend on the sensitivity of the instrument but on the accuracy of the prior and on the consequent linearization of the RT. After switching to the same version of RTTOV the results better support this explanation. Please refer to the replies n. 2 and 32 to the second referee for a more detailed discussion on this point.

2. *ECMWF NWP forecasts are used in both SOFRID and CTM assimilation. In the CTM runs, forecasts are taken from the latest available analysis (00 or 12 UTC) as said in sec. 3.1, supposedly every hour, and scaled on the CTM grid. In the SOFRID retrieval process, are the forecasts from IFS used the same way? Before being fed to RTTOV, the meteorological forecasts have to be interpolated to the location of IASI pixels. I would appreciate that the authors describe how this*

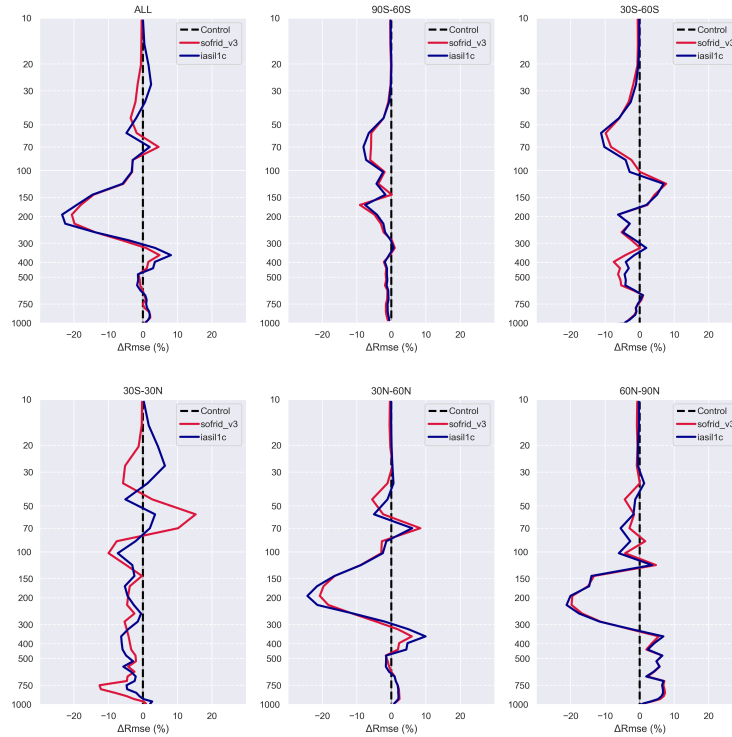


Figure 2. Relative difference of RMSE (Δ RMSE) with respect to radiosoundings for L1a (blue) and L2a (red). The difference is computed by subtracting the RMSE of L1a (L2a) against radiosoundings from the RMSE of the control simulation. Negative values mean that the assimilation improved (decreased) the RMSE of the control simulation, positive values indicate degradation (increase) of the RMSE. The same pixels selection of the original manuscript is used to produce this figure. The only difference with the original manuscript is that SOFRID v3.0 retrievals are used instead of v1.6 (Tab. 1).

Table 1. Versions of SOFRID used for the original and revised manuscript.

SOFRID Version	T and H2O	Cloud factor	RTTOV version	Usage
1.5 (Barret et al., 2011)	EUMETSAT L2	EUMETSAT plus L1	9.0	Original manuscript (only cloud factor)
1.6	ECMWF NWP	L1	9.0	Original manuscript (except cloud factor)
3.0	ECMWF NWP	EUMETSAT plus L1	11.1	Revised manuscript

interpolation is done in SOFRID and in the CTM. ECMWF 4DVAR analyses have ozone in the control variable and assimilate ozone-sensitive information (such as some IASI channels). I would not be surprised that the subsequent ECMWF forecasts are more consistent with the L1 assimilation than with the L2 products. Can the authors elaborate on that point?

5 **Answer:**

The meteorological forcing of MOCAGE is retrieved from the ECMWF MARS servers with a 3 hours stepping (available steps for the forecast type “fc”), further regridded to the CTM resolution ($2^\circ \times 2^\circ$) and stored as input files. During the MOCAGE execution the meteorological fields are interpolated linearly at hourly sub-steps, which corresponds to the advection time step of the CTM, and vertically (91 to 60 levels, linear interpolation). The observation operator performs an additional bi-linear interpolation at the position of each observation and a linear interpolation to the observation’s time. The obtained profiles (temperature, water vapor and ozone on the CTM levels) are used to feed RTTOV, which is in charge of the final vertical interpolation to the coefficients levels. As a consequence, both the spatial and temporal resolution of the RTM vertical profiles are degraded with respect to the original NWP forecasts but are coherent with the resolution of the CTM model. On the other hand, surface properties such as surface skin temperature, which are only needed for the RT and might display a larger variability at smaller scales than the CTM resolution are taken from higher resolution IFS fields ($0.125^\circ \times 0.125^\circ$) and interpolated at the IASI pixel using nearest neighbor approach.

SOFRID preprocessor retrieves the IFS operational analysis (type “an”) at 00-06-12-18 UTC, regridded to a resolution of $0.25^\circ \times 0.25^\circ$. All the fields are then interpolated at the closest hour to the IASI pixel and a nearest neighbor interpolation is done to extract the corresponding profiles and surface properties. These information have been added to the revised manuscript (Sec. 2.1.2 and 3.1) and Table 1 (now Table 2 in the revised manuscript) was upgraded accordingly.

Hence, differences between L1a and L2a due to the different origin, resolution and interpolation of the temperature and water vapor profiles might contribute to differences observed in our results. However, we assimilated the IASI main ozone window in the study ($980\text{-}1100\text{ cm}^{-1}$) and channels with strong sensitivity to water vapor were excluded both in L1a and L2a (Sec. 2.4). Therefore, we expect the impact of the meteorological profiles on our results to be minor. To confirm this we rerun all the experiments of the manuscript using ERA interim instead of the operational NWP forecasts to force the CTM. ERA interim not only differs in the model configuration with respect to the NWP operational model (e.g. 60 vertical levels for ERA interim versus 91 for the NWP model in 2010), but also for the assimilation: for example no IASI data are assimilated within ERA interim. This introduces some differences in the RTM computations for L1a but also in the control O_3 fields through the CTM forcing, thus requiring to recompute L1a, L2a and the control simulation. Since L2 products are kept the same, potential differences between L1a and L2a due to the meteorological profiles are now amplified. We show in Fig. 3 the same plots as in Fig. 6 (and revised manuscript) but computed using ERA interim forcing. The differences between L1a and L2a at the tropics show similar patterns to previous results and suggest that the main results of this study are not a consequence of the different meteorological profiles. We kept the original choice for the meteorological profiles in the revised manuscript and added a sentence to discuss this point (page 14, line 20).

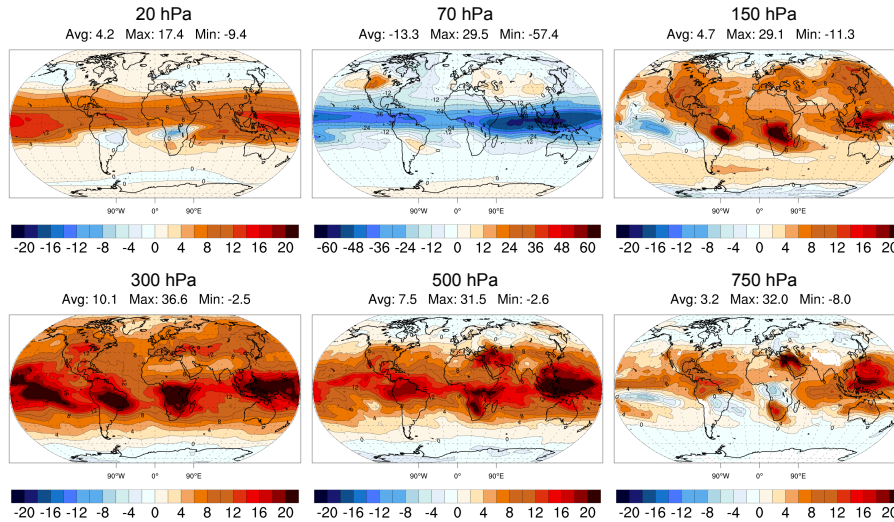


Figure 3. Relative differences (%) between radiances and Level 2 assimilation (same plots as in Fig. 6) but forcing the CTM with ERA-interim analyses instead of ECMWF operational forecasts.

The surface skin temperature has a strong signature in the IASI O_3 window and, even if it is included in the control vector, the different background values used in SOFRID and L1a might have an impact on our results. Hence, we replaced the surface skin temperature used originally in L1a (IFS 3-hourly forecasts at $0.125^\circ \times 0.125^\circ$) with the one already used in SOFRID (IFS 6-hourly analysis at $0.25^\circ \times 0.25^\circ$). Results in Fig. 4 show that the choice of the background skin temperature has not a significant impact on our results. We kept the original choice in the revised manuscript and added a sentence to discuss this point (page 14, line 18).

We do not fully understand the referee's comment about the "better consistency of L1 assimilation with ECMWF forecasts than L2 products": even if some IASI ozone channels are assimilated in IFS, we do not make any use of ozone fields from NWP forecasts in our study. Hence, we do not expect any particular advantage for L1 assimilation compared to L2 assimilation due to the meteorological forcing itself. Conversely, the fact that SOFRID (v1.6 and 3.0) uses the IFS analyses should in principle make SOFRID background radiances closer to L1 observations than the CTM ones, which uses instead forecast fields (also at a degraded spatial resolution).

3. *No description of the L1 and L2 innovation statistics is given. Figures on biases and standard deviations of L1 and L2 innovations would be of interest in this paper. How the value chosen for the observation error standard deviation ($0.7 \text{ mWm}^{-2}\text{sr}^{-1}$) compare to those statistics? Cloud masks are not really described. Cloud fraction from AVHRR is mentioned but no threshold value is given. How clear cases are selected? A data thinning is applied. Which is the minimum distance between two pixels? No description of the spatial coverage of L1 and L2 is given. Would it be possible to have a typical daily coverage or an average density over the month?*

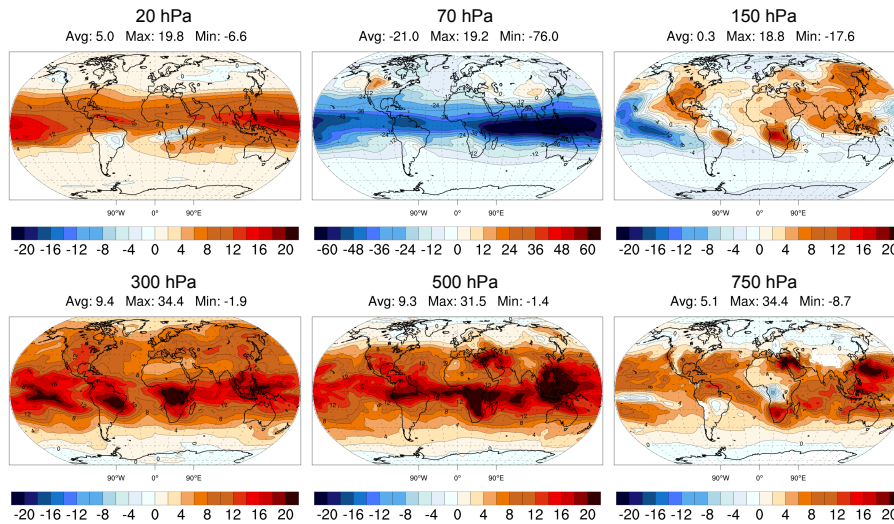


Figure 4. Relative differences (%) between radiances and Level 2 assimilation (same plots as in Fig. 6) but using exactly the same background surface skin temperature for L1 assimilation and L2 retrievals.

Answer:

The answer to this question is split in two parts.

Innovation statistics: The innovation statistics represent one of the main diagnostics of data assimilation experiments and have been carefully evaluated during the study. We report for example in Fig. 5 the average innovations of L1 assimilation (experiment L1a) for the entire month of July 2010. We remark for example that the biases of the control simulation are moderate (about $1 \text{ mWm}^{-2}\text{sr}^{-1}\text{cm}$) and that the background (forecast) innovation in the middle of the spectral window is smaller than on the tails. The latter is likely due to the different spectral contributions of ozone and skin temperature and the fact that the skin temperature is not a prognostic variable of the CTM (i.e. the background SST is the same in the control and in the forecast). The value of the observation error was deliberately fixed equal to the one used for L2 retrievals to compare L1a and L2a for same settings. Improvements of the observation error covariance, potentially with the aid of more detailed innovation analysis, are left for a future study (page 15, line 22 of the original manuscript). Even though this type of plots contain highly valued information, we prefer not including them since they are not essential for the conclusions of this study and to avoid an excessive length of the manuscript. Moreover, L1 and L2 innovations are not directly comparable because of their different nature (radiance and profiles).

Preprocessing method: the results in Fig. 1 and 2 of this document have been obtained assimilating exactly the same satellite pixels as in the original manuscript, and were shown here to highlight differences due only to the RTTOV version. These pixels were selected based on a combination of cloud masks from an older version of SOFRID (v1.5, see Tab. 1 and description in Sec. 2.1, page 5, line 15) and AVHRR cloud mask available only in most recent L1c files.

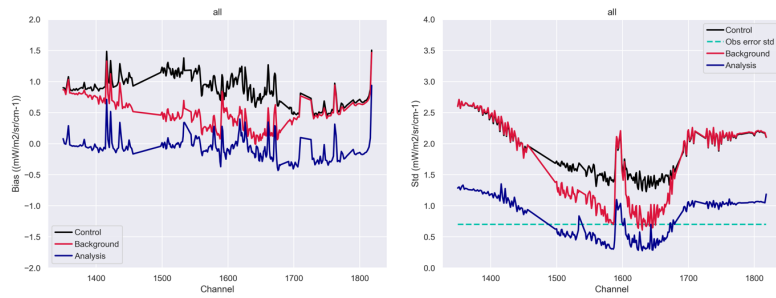


Figure 5. Average (left) and standard deviation (right) of the L1 innovations for the entire period of simulation. The control line represents the innovation with respect to the control simulation (no DA). The dashed turquoise line represents the observation error standard deviation used for the SOFRID retrievals and L1a experiments.

Due to the different data processors these cloud masks are not the same. For both data sources only pixels with a cloud factor smaller than 1% were first selected. The information was given at page 6, line 18 of the original manuscript. The resulting datasets were colocated to ensure that a valid SOFRID retrieval was available for each L1c pixels. Finally, a data thinning was performed hourly: we covered the Earth with a $1^\circ \times 1^\circ$ grid and within an hourly loop we retained only the first satellite pixel found within every two grid boxes. A minimum distance of 1° before assimilated pixels is therefore ensured. Overall, the selection resulted in about 3300 pixels per day for the assimilation, as mentioned in Sec. 2.4 of the original manuscript.

With version v1.6 (the retrievals assimilated in the original manuscript), SOFRID was upgraded to use water vapor and temperature profiles from IFS instead of EUMETSAT L2 retrievals (Tab. 1). This increased the number of retrieved pixels with respect to v1.5, since SOFRID was not subject anymore to the availability of the EUMETSAT Level 2. On the other hand, the original cloud mask of v1.5 based on both L1 spectra and EUMETSAT processor was replaced by the L1-only based mask (described in Sec 2.2 of Barret et al. (2011)). To avoid possible cloud contamination the best option was then to keep the original pixel selection done initially with SOFRID v1.5 but using the retrievals from v1.6. Therefore, all results presented in the original manuscript were based on about 3300 assimilated observations per day (page 6, line 22).

With SOFRID v3.0 (RTTOV 11) the EUMETSAT cloud mask was reintroduced in the L2 product, and allowed to apply the full preprocessing procedure described above but using only v3.0 files. At the end, this resulted in an increased number of pixels available for each day to about 5000 (Fig. 8). Differences between L1 and L2 assimilation are enhanced due to the higher number of assimilated observations (Fig. 6 and 7), but show the same patterns as in Fig. 1 and 2. We retained this configuration for the revised manuscript, we extended the description of data thinning (page 7, line 25) and we included a new plot showing the number of assimilated observations per grid point during the simulation period (Fig.

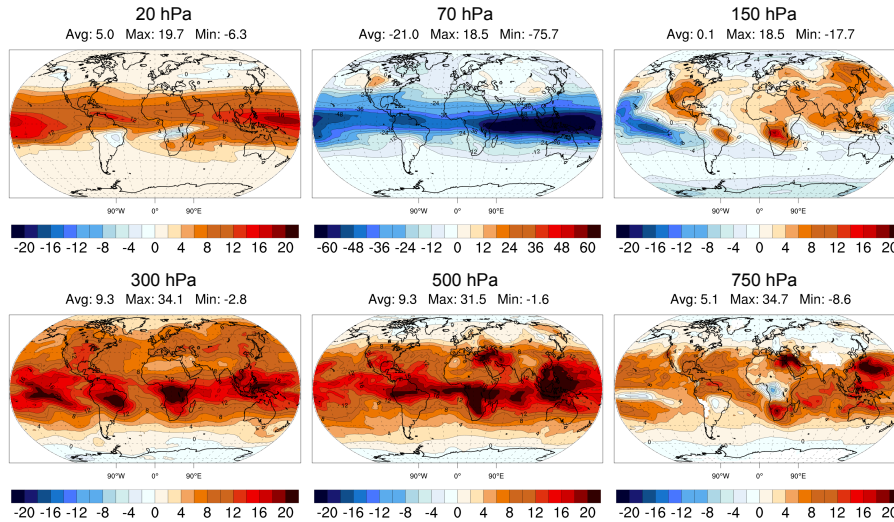


Figure 6. Relative differences (%) between radiances and Level 2 assimilation (same plots as in Fig. 1) but using the new set of colocated observations (right plot in Fig. 8) and SOFRID V3.0 (RTTOV 11). This figure replaces Fig. 2 of the original manuscript.

8, right plot). All figures in this document (except Fig. 1 and 2) and in the revised manuscript are based on this new set of experiments with increased number of observations.

4. *Background covariance error matrix: the values used in this study (2% / 10%) are barely supported by Figure 1. The authors state that the bias may be an important component of the RMSE in Figure 1, is it possible to provide profiles of bias and standard deviation in addition to RMSE? P10 L5, the vertical structure of the B matrix is described as "correlation length of 1 model grid point". Do you mean 1 model level? Please clarify.*

Answer:

We extended Figure 1 with the full validation statistics of the control simulation (bias, standard deviation and RMSE), which are reported here in Fig. 9,10 and 11 respectively. The validation values obtained against MLS are also added to these plots for completeness. We remark that biases can be as high as 30% close to the tropopause and that standard deviation and RMSE values relative to MLS are generally smaller due to the increased accuracy and number of MLS observations. Even if we consider MLS lines as reference for the stratosphere, the values chosen for the background standard deviation may still seem small with respect to those in Fig. 10. However, the assimilation background is more accurate than the control simulation (Fig. 12 for the MLSa forecast), with RMSE values that fell generally below 5% in the stratosphere. We also remind that we neglected the radiances error correlation in our study. This leads to a stronger weight of the assimilated observations, that we compensated by smaller values of the background error covariance. Values of 5%-25% for the standard deviation in the stratosphere and troposphere respectively lead typically to worse

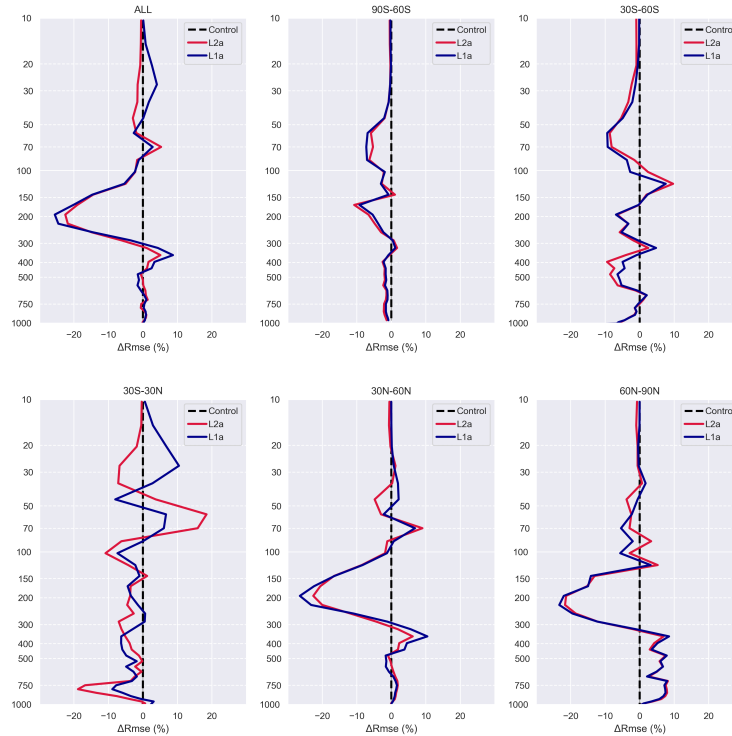


Figure 7. Relative difference of RMSE (Δ RMSE) with respect to radiosoundings for L1a (blue) and L2a (red) (same plots as in Fig. 2) but using the new set of colocated observations (right plot in Fig. 8) and SOFRID V3.0 (RTTOV 11). This figure replaces Fig. 3 of the original manuscript.

reanalyses (not shown). Using a relatively small error in the stratosphere (2%) mitigated the issues encountered with IASI assimilation (L1 and L2) and did not reduce significantly the positive impact of MLS.

This study is focused on comparing L1 and L2 assimilation with identical values for B: we think that the empirical choices for the B matrix are satisfactory for the objective of the study. Further optimization of B and R, which is often done simultaneously (Desroziers et al., 2005), is left for a future study, where non-diagonal terms of R should also be included in L1 assimilation. We extended the discussion of the background error covariance to include elements from this reply and the reply n 24 to the second reviewer (page 12, lines 6 and 12). We also precised that the scale of the vertical error correlation is expressed in number of model levels (page 13, line 1).

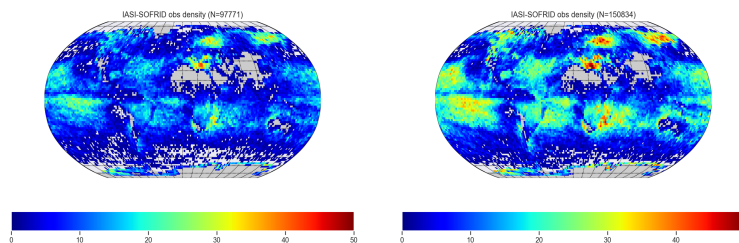


Figure 8. Number of assimilated observations for each model grid point ($2^\circ \times 2^\circ$) and for the entire simulation period (July 2010). Number of observations used in the original manuscript on the left (SOFRID 1.6) and for the revised manuscript on the right (SOFRID 3.0). The total number of observations is displayed on the top of each plot.

5. *Results L1 vs L2* Figure 2 shows the relative differences between L1 analyses and L2 analyses. As the values of background error variances are rather small, I would find interesting to show analysis increments difference statistics (average and/or standard deviation). All figures are given in relative difference and no ozone fields are plotted. Except from the value given P11 L6, the reader have no idea how these relative differences compare to the actual ozone concentration. I would appreciate the authors find a way to illustrate the 3D field they want to analyze in their study. Figure 3 (and similar figures) would be more useful if error bars were added. They would help understand whether the differences are statistically significant or not. The statistics are given over the whole month. How stable are they on a day to day basis? Would it be interesting to split the statistics between day and night? The paragraph about the computational cost and convergence issues is interesting but may be placed separately from the scientific results.

10 **Answer:**

The answer is split in 3 parts.

15 Increments, like innovations, are the direct output of the variational minimization and are among the first diagnostics that we looked at. Examples of increments for the third assimilation window (2010-07-01 03 UTC) are shown in Fig. 13 and 14, which confirms that the absolute increment values are significant in term of typical ozone concentrations (Fig. 15). However, while this type of plots is very meaningful to verify the correct functioning of the DA system, we found not relevant to report average increments in the manuscript. With hourly DA windows the increments are equal to zero most of the time on the global grid due to the moving observation network. Hence, averaged increments do not give valuable information in terms of absolute or relative values. Weighting the average based on the satellite overpasses is not straightforward. On the other hand, the cumulative effect of all increments during the evaluation period is well represented by the analysis fields, which is also the only field that we validated against independent measurements. We think that presenting only the analysis statistics is the best choice for the objective of our study and to avoid an excessive length of the manuscript.

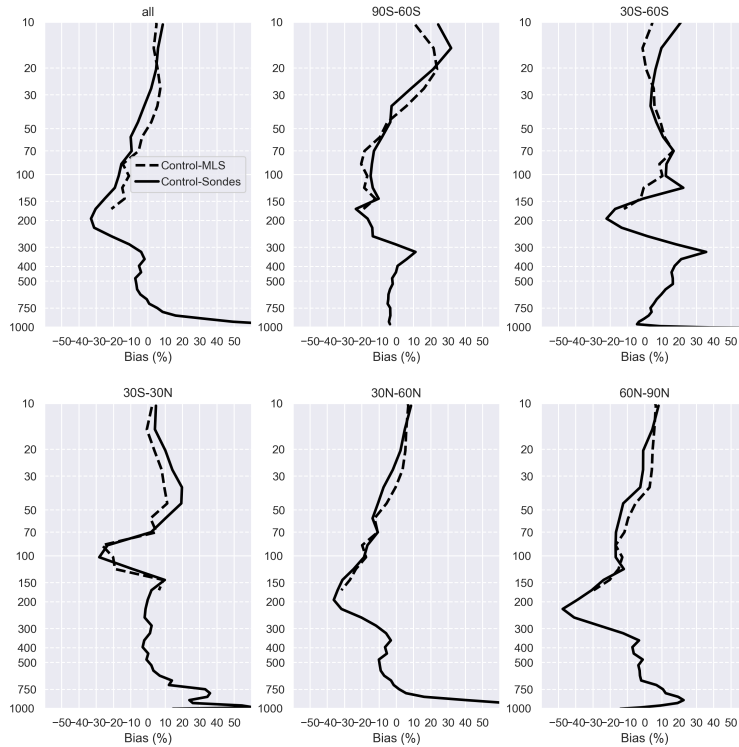


Figure 9. Relative bias of the control simulation with respect to radiosoundings (solid line) and MLS (dotted line) averaged globally (first plot) and for five latitude bands separately (90°S-60°S, 60°S-30°S, 30°S-30°N, 30°N-60°N, 60°N-90°N).

We chose to display only relative differences and relative improvements because ozone varies on an exponential scale. When showing absolute values it is often difficult to appreciate the impact of data assimilation on both the troposphere and the stratosphere, especially when examining differences between similar assimilation experiments. We report in Fig. 15 the average value of ozone of the control simulation, which are used to scale all the maps presented in the study. This figure has been included and commented in the revised manuscript (Sec. 4.1).

5

Figure 3, 4 and 6 of the original manuscript (and Fig. 2,7 in this document) represent differences of RMSE between the analyses and the control simulation. The RMSE for each simulation (e.g. Fig. 11 for the control simulation) is based on the differences between modeled and observed values for the ensemble of the observations, or for a selection based on latitude. It is not clear to us how to put error bars on such statistics. The statistical significance depends on the number of observations used to compute the various RMSEs, which are reported now in Table 2 and included in the

10

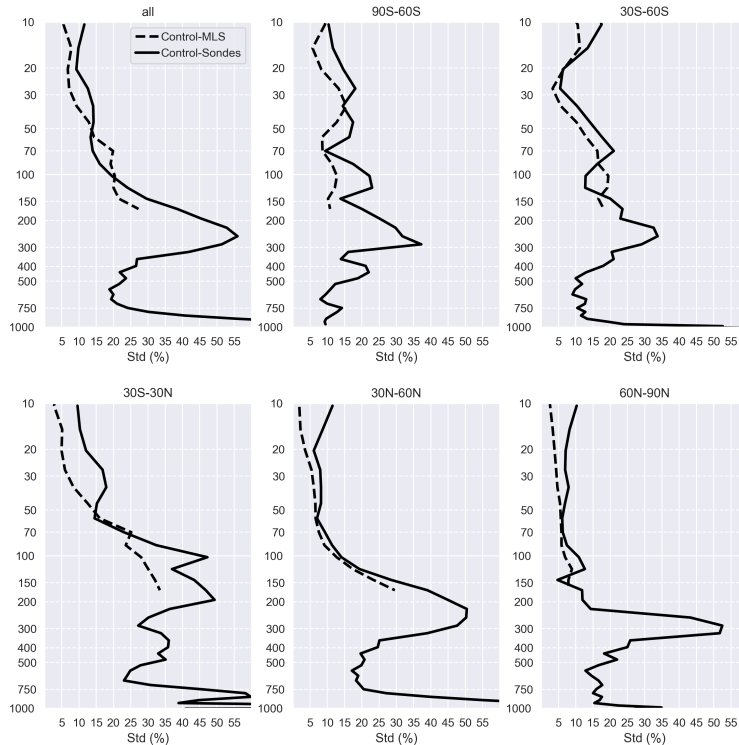


Figure 10. Relative standard deviation of the control simulation. Same plots as in Fig. 9.

revised manuscript for completeness. By looking at observation numbers we recognize that daily RMSE statistics would be difficult to compute for radiosoundings due to a too small number of observations. Similar issues arise if we try to separate between day and night, since radiosoundings are mostly launched at local noon. On the other hand, MLS allows to compute daily or night/day statistics.

5 We present in Fig. 16 the same plots as in Fig. 4 of the original manuscript but for five different days during the simulation period. We remark that the RMSE display a tendency during the period, with a slow degradation towards the end of the period. We suppose that, without MLS joint assimilation, some errors are continuously injected by IASI, especially in the case of L1a. This points to some unresolved issues with the inversion of radiances, which is probably exacerbated in L1a because of the propagation of the O_3 prior in time. An evaluation of the results over a longer period seem necessary
 10 to draw more robust conclusions on this issue. However, thanks to the MLS assimilation, this issue has a limited impact on the main results of the study.

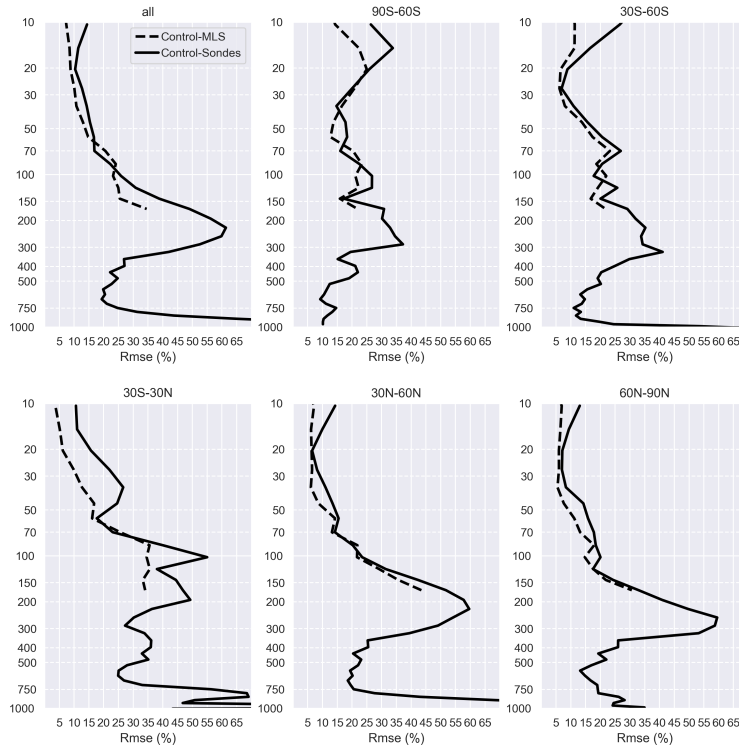


Figure 11. Relative Root Mean Square Error (RMSE) of the control simulation. Same plots as in Fig. 9.

Fig. 17 reports the RMSE statistics for the full period but split between day and night. The day-night separation is computed based on the local sun position at the time of the observation. We remark that some differences appear only at high latitudes (90°S - 60°S and 60°N - 90°N), but since the number of day-night observations changes dramatically in these regions (e.g. from 15755 to 1212 at 90°S - 60°S), a robust interpretation of these differences looks problematic.

- 5 The paragraph on the computational cost has become an independent section in the revised manuscript (Sec. 4.2).
6. *Results when MLS is assimilated* As in a real system, several sources of observation may be assimilated simultaneously, this section has a real added value. I regret that the results are not shown in a consistent way with the previous section. Figure 2 shows L1a - L2a; Figure 5 should show MLS+L1a - MLS+L2a because we want to compare these two settings.

Answer:

- 10 We agree with the reviewer and the previous figure has been replaced in the revised manuscript with MLS+L1a - MLS+L2a (Fig. 18). The new plot shows that differences are largely reduced in the stratosphere, thanks to MLS, but

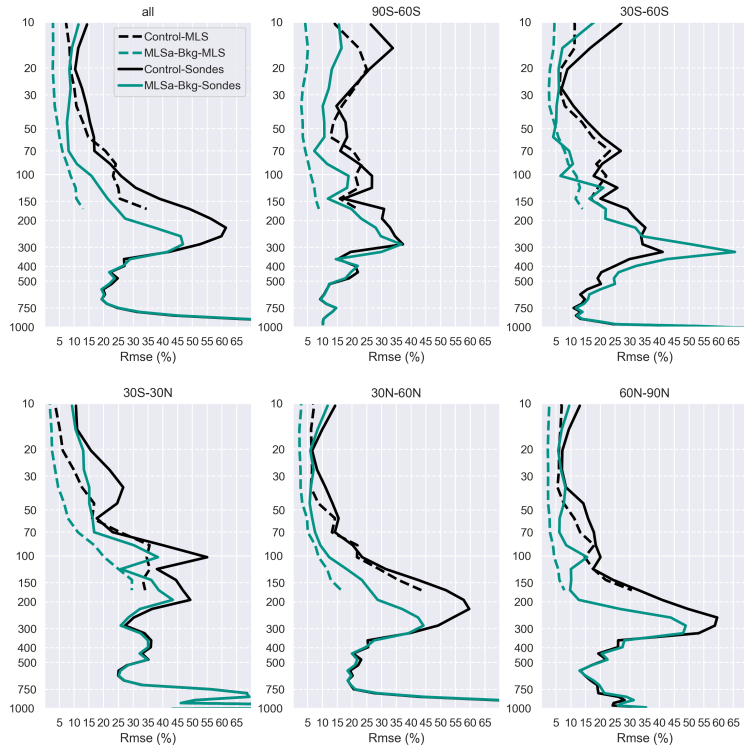


Figure 12. Relative Root Mean Square Error (RMSE) of the control simulation (black lines) and of the MLSa forecast (green lines). Same plots as in Fig. 11.

Table 2. Number of validation observations.

Latitudes	MLS	Radiosoundings
Global	100975	219
90°S-60°S	16967	19
60°S-30°S	17334	9
30°S-30°N	33046	38
30°N-60°N	16669	138
60°N-90°N	16959	15

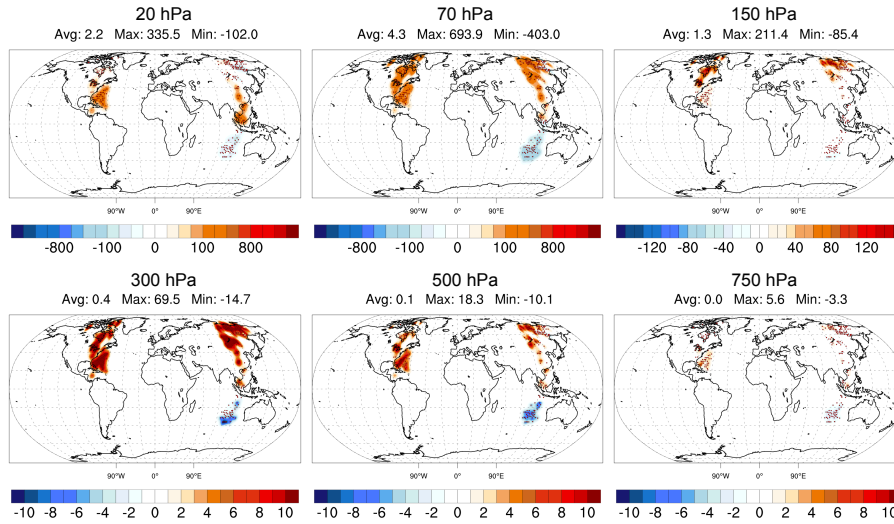


Figure 13. Absolute O₃ increments (ppb units) in L1a experiment for the 2010-07-01 03 UTC window and at different pressure levels in the stratosphere (top plots) and in the free troposphere (bottom plots).

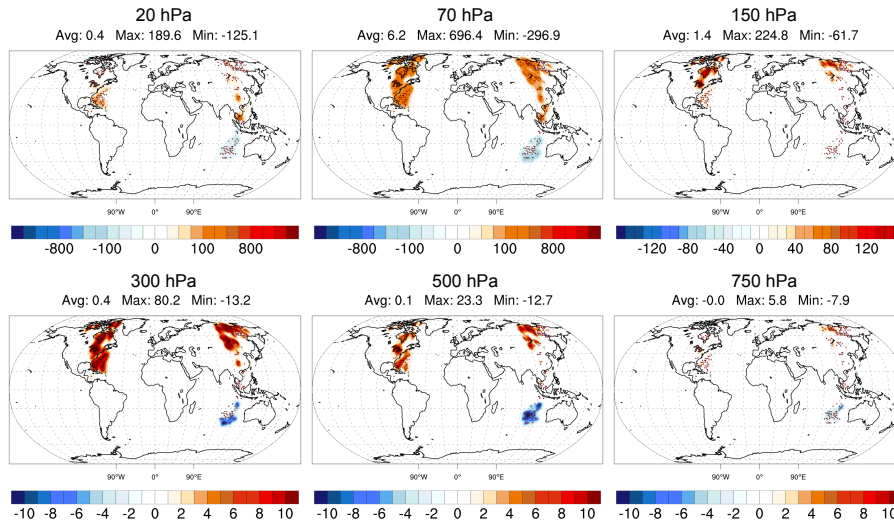


Figure 14. Absolute O₃ increments (ppb units) in L2a experiment for the 2010-07-01 03 UTC window and at different pressure levels in the stratosphere (top plots) and in the free troposphere (bottom plots).

are still significant in the free troposphere, although to a lesser extent than for L1a-L2a (Fig. 6). As a consequence, the discussion of the previous figure has also been removed from the revised manuscript.

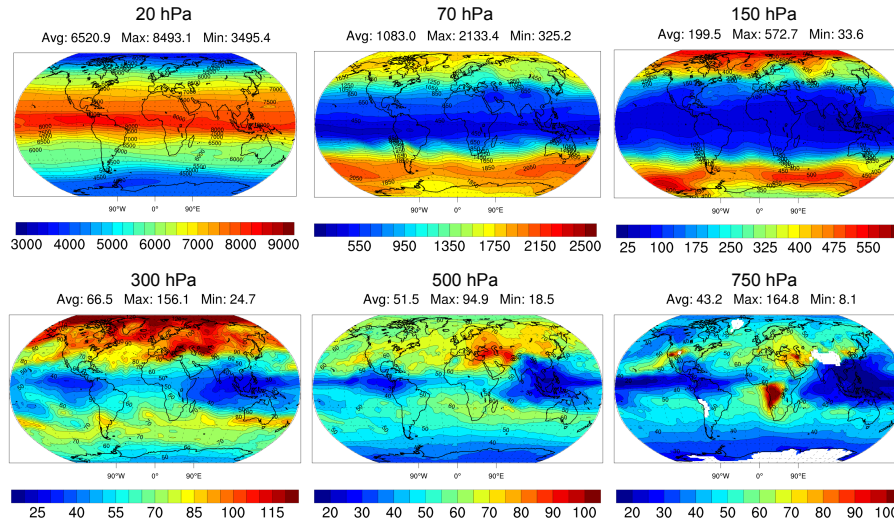


Figure 15. O₃ fields (ppb units) issued from the control simulation averaged on July 2010. From left to right different pressure levels are displayed covering the stratosphere (top) and the free troposphere (bottom). Average, maximum and minimum values of the displayed fields are given on top of each map.

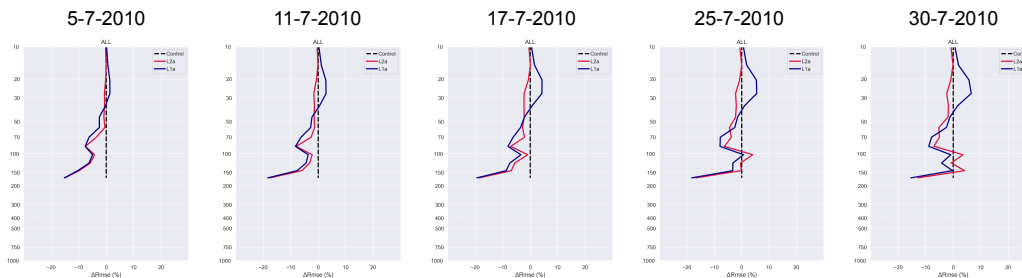


Figure 16. Gain of RMSE (Δ RMSE) computed with respect to MLS for L1a (blue) and L2a (red). Same plots as in Fig. 4 of the original manuscript but shown only for the global average and for five different dates.

2 Reply to specific comments

Answer:

All specific comments have been integrated in the revised manuscript.

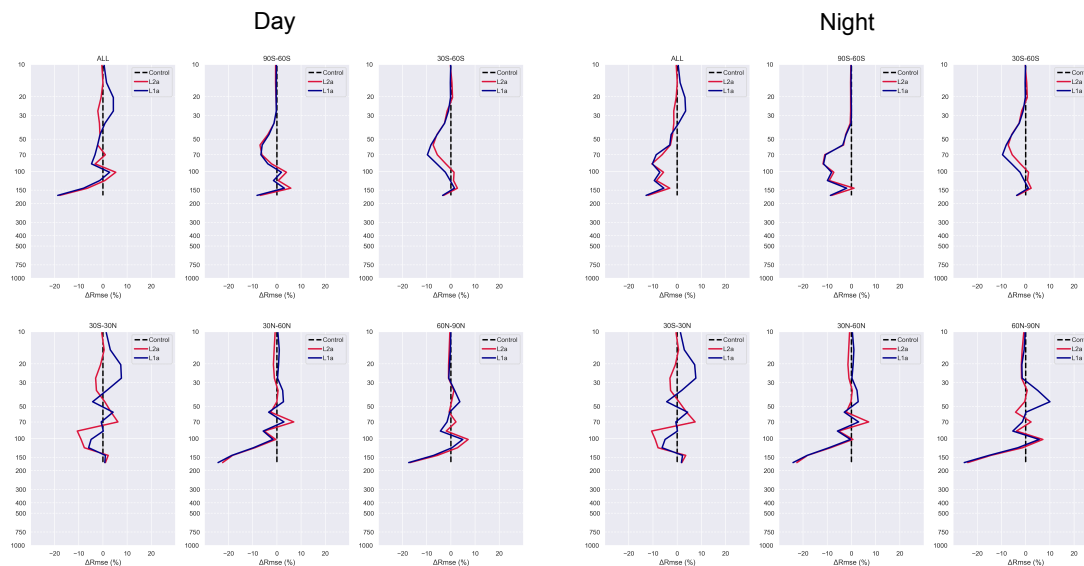


Figure 17. Gain of RMSE (Δ RMSE) computed with respect to MLS for L1a (blue) and L2a (red). Same plots as in Fig. 4 of the original manuscript but computed using only observations during daylight (left panel) and night (right panel).

References

- Barret, B., Le Flochmoen, E., Sauvage, B., Pavelin, E., Matricardi, M., and Cammas, J. P.: The detection of post-monsoon tropospheric ozone variability over south Asia using IASI data, *Atmospheric Chemistry and Physics*, 11, 9533–9548, <https://doi.org/10.5194/acp-11-9533-2011>, <http://www.atmos-chem-phys.net/11/9533/2011/>, 2011.
- 5 Desroziers, G., Berre, L., Chapnik, B., and Poli, P.: Diagnosis of observation, background and analysis-error statistics in observation space, *Quarterly Journal of the Royal Meteorological Society*, 131, 3385–3396, <https://doi.org/10.1256/qj.05.108>, <http://doi.wiley.com/10.1256/qj.05.108>, 2005.

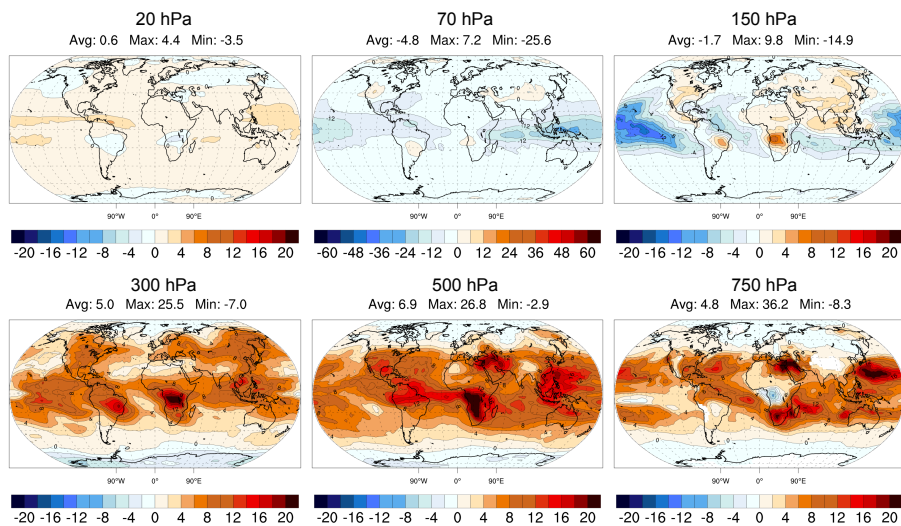


Figure 18. Relative differences (%) between L1a+MLS minus L2a+MLS divided by the correspondent O_3 values of the control simulation averaged on July 2010. From left to right different pressure levels are displayed covering the stratosphere (top) and the free troposphere (bottom). Average, maximum and minimum values of the displayed fields are given on top of each map. This figure replaces Fig. 5 of the original manuscript.